

## Valence-band ordering in ZnO

D. C. Reynolds, D. C. Look, and B. Jogai  
Semiconductor Research Center, Wright State University, Dayton, Ohio 45435

C. W. Litton  
Materials and Manufacturing Directorate, Air Force Research Laboratory, Wright-Patterson Air Force Base, Ohio 45433

G. Cantwell and W. C. Harsch  
Eagle-Picher Industries, Inc., 200 B. J. Tunnell Boulevard, Miami, Oklahoma 74354  
(Received 14 May 1998; revised manuscript received 9 March 1999)

The emission and reflection spectra of ZnO have been investigated in the intrinsic region and the data have been interpreted in terms of the wurtzite crystal band structure. Free-exciton emission is observed for the first time. Both the  $\Gamma_5$  and  $\Gamma_6$  state excitons associated with top valence band have been identified. This identification has established the valence-band symmetry ordering in ZnO. [S0163-1829(99)14727-1]

### INTRODUCTION

There has been a long standing controversy over the symmetry ordering of the valence bands in ZnO. ZnO crystallizes stably in the wurtzitic modification and the wurtzitic band structure was first derived by Birman.<sup>1</sup> The zone-center conduction band is *s* like having  $\Gamma_7$  symmetry. The valence band is *p* like, splitting into three doubly degenerate bands due to spin-orbit and crystal-field interactions. The top valence band, *A*, has  $\Gamma_9$  symmetry while the two lower valence bands, *B* and *C*, have  $\Gamma_7$  symmetry. The fundamental exciton spectra of ZnO crystals were first investigated by Thomas.<sup>2</sup> From reflection spectra, he identified three exciton series, one associated with each of the three valence bands. From polarization studies of both reflection and absorption spectra, Thomas concluded that states from the first and third valence bands were mixed and that the symmetries of the two top valence bands were reversed with respect to the usual ordering of the wurtzitic band structure.

A later study of the exciton structure in ZnO was conducted by Park *et al.*<sup>3</sup> The essential difference between the work reported by Park *et al.*<sup>3</sup> and that of Thomas<sup>2</sup> was spectral peak assignments. The line interpreted by Thomas as the intrinsic ground state *A*—exciton transition was interpreted by Park *et al.* as an extrinsic, ionized donor-bound exciton complex transition. Thus, from their studies, Park *et al.* concluded that the valence-band symmetry ordering in ZnO was not reversed, as was claimed by Thomas.

Recently ZnO crystals have become available in which intrinsic exciton transitions are observed in emission. This has provided additional information relative to the exciton structure of ZnO. The present study has emphasized specific optical transitions that are pertinent to identifying the valence-band ordering. Let us consider emissive optical transitions from the  $\Gamma_7$  conduction band to the  $\Gamma_9$  valence band, or conversely, absorptive transitions from the  $\Gamma_9$  valence band to the  $\Gamma_7$  conduction band. From group theoretic arguments and the direct product of the group representations of these band symmetries, we obtain the following intrinsic ex-

citon ground-state symmetries for either emissive or absorptive processes

$$\Gamma_7 \times \Gamma_9 \rightarrow \Gamma_5 + \Gamma_6.$$

The  $\Gamma_5$  and  $\Gamma_6$  exciton ground states are both doubly degenerate; the  $\Gamma_5$  exciton transition is allowed, whereas the  $\Gamma_6$  exciton transition is forbidden. In the  $\Gamma_5$  exciton, electron and hole spins are paired, while in the  $\Gamma_6$  exciton they are parallel. In this investigation, the polarization and magnetic field properties of these two intrinsic excitons have been carefully studied.

Let us now consider emissive optical transitions from the  $\Gamma_7$  conduction band to the  $\Gamma_7$  valence band and converse optical-absorption processes. For such transitions, one obtains the following exciton symmetries and states

$$\Gamma_7 \times \Gamma_7 \rightarrow \Gamma_5 + \Gamma_1 + \Gamma_2.$$

The  $\Gamma_5$  exciton state is doubly degenerate and the  $\Gamma_1$  and  $\Gamma_2$  exciton states are both singly degenerate. Transitions from the  $\Gamma_5$  and  $\Gamma_1$  exciton states are allowed while those from the  $\Gamma_2$  exciton state are forbidden. The magnetic-field behavior of excitonic optical transitions from the  $\Gamma_7$  conduction band to the  $\Gamma_7$  valence band is very different from that of excitonic transitions from the  $\Gamma_7$  conduction band to the  $\Gamma_9$  valence band. It is this difference in magnetic-field behavior between  $\Gamma_7 \rightarrow \Gamma_7$  and  $\Gamma_7 \rightarrow \Gamma_9$  excitonic transitions that is used in the present study to resolve the valence-band ordering in ZnO. We conclude that the *A*-exciton transition identified by Thomas is indeed an intrinsic exciton, but that the valence-band symmetry ordering in ZnO is, nevertheless, *A*- $\Gamma_9$ , *B*- $\Gamma_7$ , *C*- $\Gamma_7$ , identical to that observed in most other II-VI wurtzitic structures, as well as in wurtzitic GaN.

### EXPERIMENTAL DETAILS

The high-quality ZnO samples were cut from a 2-inch boule grown by a seeded physical vapor transport method. Photoluminescence (PL) spectral measurements were made at 2 K with the sample immersed in liquid He. PL excita-

TABLE I. Comparison of expected exciton transitions, under various symmetries of the top valence band.

CB	VB	Excitons	$E\parallel c, H\parallel c$		$E\perp c, H\parallel c$	
			$H=0$	$H$	$H=0$	$H$
			Oscillator Strength	$g$ -Value	Oscillator Strength	$g$ -Value
$\Gamma_7$	$\Gamma_9$	$\Gamma_5$	+Weak	$g_e - g_h$	*A	$g_e - g_h$
		$\Gamma_6$	Weak	$g_e + g_h$	Weak	$g_e + g_h$
$\Gamma_7$	$\Gamma_7$	$\Gamma_5$	Weak	$g_e + g_h$	A	$g_e + g_h$
		$\Gamma_1$	A	0	Weak	0
		$\Gamma_2$	Weak	0	Weak	0

\*"A"-denotes an allowed transition.

+ "Weak"-unallowed transitions that can be weakly observed due to misalignment, local strains, or  $k \neq 0$  transitions (since the photon has a finite momentum).

tion was achieved with the 3250 Å line of a He-Cd uv laser. The reflectivity measurements were also made at 2°K using a high-pressure Xe arc lamp source, which provided ample continuum in the spectral region of interest. The crystal was mounted on a copper holder with the "c" axis of the crystal oriented parallel to the long axis of the rectangular holder. Both the PL and reflectivity spectra were analyzed by means of a high-resolution 4-meter grating spectrometer equipped with an RCA C31034A photomultiplier tube for detection.

## EXPERIMENTAL RESULTS

We first consider the free-exciton emission spectra, with and without a magnetic field  $H$  parallel to the  $c$  axis ( $H\parallel c$ ), and with the electric-field vector either parallel ( $E\parallel c$ ) or perpendicular ( $E\perp c$ ) to the  $c$  axis. We will attempt to distinguish between the two possible symmetry assignments ( $\Gamma_9$  or  $\Gamma_7$ ) for the top valence band. The properties of the expected exciton lines, for each symmetry, are summarized in Table I.<sup>4</sup> The experimental data for the case  $E\parallel c$  and  $H\parallel c$  are presented in Fig. 1. If the top valence band is of  $\Gamma_9$  symmetry, then two exciton lines ( $\Gamma_5$  and  $\Gamma_6$ ) should appear at finite  $H$ , but both should be weak or nonexistent at  $H=0$ . In

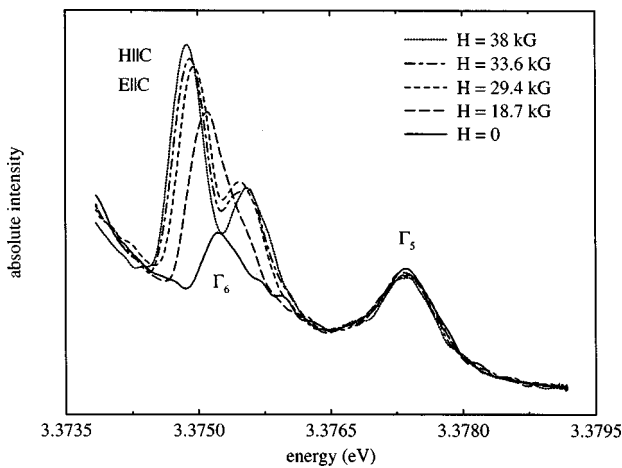


FIG. 1. Second order PL showing the  $\Gamma_5$  and  $\Gamma_6$  excitons in zero-magnetic field as well as in applied fields  $H\parallel c$ ,  $E\parallel c$ .

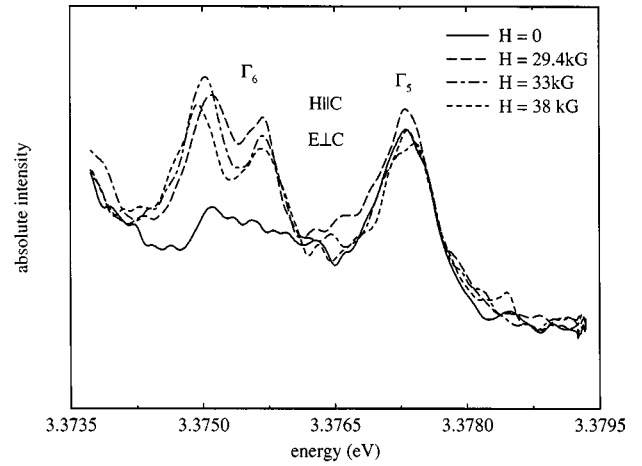


FIG. 2. Same as Fig. 1 except the orientation is now  $H\parallel c$ ,  $E\perp c$ .

fact, we indeed see two weak lines at  $H=0$ , (the weak appearance of the  $\Gamma_6$  line is likely due to the finite momentum of the photon,<sup>5</sup> and that of the  $\Gamma_5$  line, to unwanted collection of light with  $E$  not exactly parallel to  $c$ ). Furthermore, at finite  $H$ , we can explain the strongly split line as  $\Gamma_6$ , and the weakly split line as  $\Gamma_5$ . These assignments result from the fact that  $\Gamma_6$  should split as the sum of the electron and hole  $g$  values ( $g_e + g_h$ ), and  $\Gamma_5$ , as the difference ( $g_e - g_h$ ). Since the  $\Gamma_6$  splitting gives  $g = 3.09$ , and since  $g_e \approx 1.95$ , from Ref. 6, we derive  $g_h = 1.14$ . This latter number agrees well with the value  $g_h = 1.2$  calculated from the Zeeman splitting of a shallow neutral-donor-bound exciton.<sup>6</sup> We next investigate the case  $E\perp c$ ,  $H\parallel c$ , shown in Fig. 2. Here the  $\Gamma_5$  line is stronger, as expected (it is now allowed), and shows little splitting, and the  $\Gamma_6$  line is still weak at  $H=0$  and splits strongly (as  $g_e + g_h$ ) at finite  $H$ . Thus, all of the data are consistent with the assignment of  $\Gamma_9$  symmetry to the top valence band, as summarized in Table I.

We now look at the possibility of  $\Gamma_7$  symmetry for the top valence band. For the case  $E\parallel c$ ,  $H\perp c$ , Fig. 1, we could assign the low-energy line to  $\Gamma_5$ , which should split as  $g_e + g_h$ , and the high-energy line to  $\Gamma_1$ , which should not split. The first problem with this model is that the energy ordering is reversed from what would be expected.<sup>2</sup> However, a more serious problem is evident when we consider the  $E\perp c$ ,  $H\parallel c$  case, Fig. 2. In this orientation, according to Table I,  $\Gamma_5$  should be strong, and  $\Gamma_1$  weak, exactly opposite to what is observed. If we, instead, assign the low-energy line at  $H=0$  to  $\Gamma_1$ , and assume that the "splitting" occurs from the appearance of  $\Gamma_2$  at finite  $H$ , the splitting would be expected to go as  $g_e - g_h$ . The high-energy line would then be a  $\Gamma_5$  exciton and should split as  $g_e + g_h$ , which is clearly not the case. Thus, we believe that the data in Figs. 1 and 2 cannot be explained by the assumption of  $\Gamma_7$  symmetry for the top valence band.

The reflection and emission spectra, extended to higher energies in the intrinsic region, are shown superimposed in Fig. 3. In this case, both the ground-state and excited-state emission from the free excitons is observed for the orientation  $E\perp c$ . From the emission spectrum, the exciton binding energies are obtained, assuming the excited states are hydrogenic. This leads to reliable band-gap energies for both the A and B bands, summarized in Table II. Note that the emission

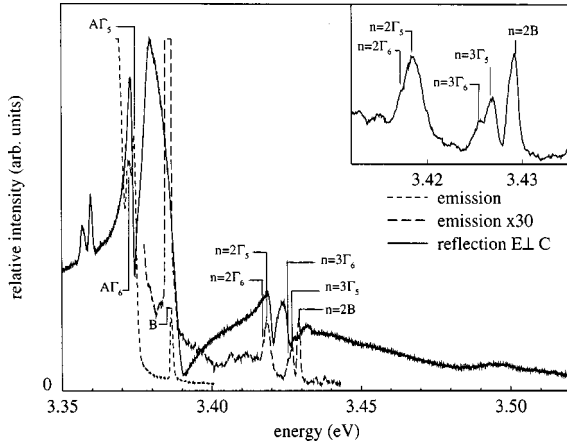


FIG. 3. Superposition of first order emission and reflection spectra. An expanded view of the excited state emission transitions is shown in the inset. The energies of the emission transitions are given in Table II.

spectrum is much more detailed than the reflection spectrum.

Emission from the *C* band is not observed; however, reflection for the orientation  $H\parallel c$  shows both the ground and first excited state of the *C* band. The reflection spectra for the orientations  $E\perp c$  and  $E\parallel c$  are shown in Fig. 4. The energies of the reflection minima are given for all three bands. Unfortunately, the reflection peaks do not directly give the oscillator energies associated with the three bands. The emission peak gives the energy of the oscillator, and exciton emission

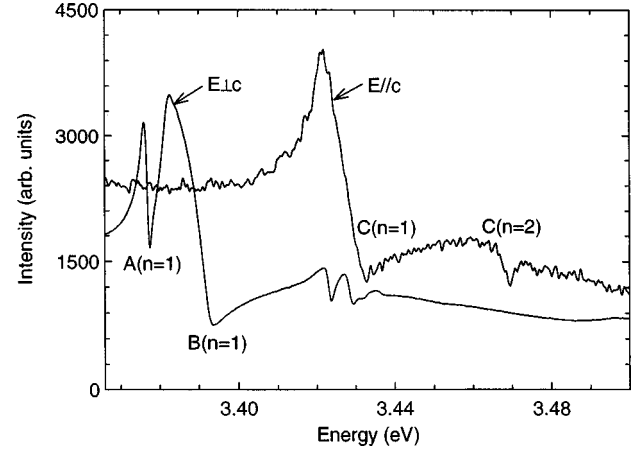


FIG. 4. Reflection spectra for the orientation  $E\perp c$  and  $E\parallel c$ . The reflection minima are as follows: *A*-exciton 3.3776 eV, *B*-exciton 3.3938 eV, *C*-exciton 3.4335 eV. *C*(*n*=2)-exciton 3.4700 eV,

is observed for both the *A* and *B* bands. From this one can obtain the energy separation of the *A* and *B* bands. One can get an estimate of the energy separation of the *B* and *C* bands from the reflection minimum of each band, if one assumes that the energy of the oscillator has the same relationship to the reflection minimum in both bands. This estimate is also reported in Table II.

The contributions of the spin-orbit interaction and the crystal-field perturbation to the experimentally observable splittings,  $E_{1,2}$  (which is the energy difference between the *A*

TABLE II. Parameters Pertinent to ZnO.

Parameters	Values	Measured PL-Spectra	Derived
<i>A</i> -Exciton $\Gamma_5$ Ground-State Energy	3.3773 eV	X	
<i>n</i> = 2 energy	3.4221 eV	X	
<i>n</i> = 3 energy	3.4303 eV	X	
Binding Energy <i>n</i> = 2	0.0597 eV		X
Binding Energy <i>n</i> = 3	0.0596 eV		X
Band Gap Energy	3.4370 eV		X
<i>A</i> -Exciton $\Gamma_6$ Ground-State Energy	3.3756 eV	X	
<i>n</i> = 2 Energy	3.4209 eV	X	
<i>n</i> = 3 Energy	3.4288 eV	X	
Binding Energy <i>n</i> = 2	0.060 eV		X
Binding Energy <i>n</i> = 3	0.0598 eV		X
<i>B</i> -Exciton Ground-State Energy	3.3895 eV	X	
<i>n</i> = 2 Energy	3.4325 eV	X	
Binding Energy	0.057 eV		X
Band Gap Energy	3.4465 eV		X
$E_{AB}, \Gamma_9 - \Gamma_7$	0.0095 eV		X
Parameters	Values	Measured Reflection Spectra	Derived
<i>A</i> -Exciton Reflection Minima	3.3776 eV	X	
<i>B</i> -Exciton Reflection Minima	3.3938 eV	X	
<i>C</i> -Exciton Reflection Minima	3.4335 eV	X	
$E_{BC}, \Gamma_7 - \Gamma_7$	0.0397 eV		X
Spin-Orbit Parameter	0.016 eV		X
Crystal-Field Parameter	0.043 eV		X

and  $B$  band gaps) and  $E_{2,3}$  (which is the energy difference between the  $B$  and  $C$  band gaps) have been calculated by several investigators.<sup>4,7-11</sup> For the case in which the wurtzite energy levels are treated as a perturbation of those in zinc blende, Hopfield<sup>4</sup> has derived the relations

$$E_1 = 0$$

$$E_2 = -\frac{\delta + \Delta}{2} + \sqrt{\left[\left(\frac{\delta + \Delta}{2}\right)^2 - 2/3\delta\Delta\right]}$$

$$E_3 = -\frac{\delta + \Delta}{2} - \sqrt{\left[\left(\frac{\delta + \Delta}{2}\right)^2 - 2/3\delta\Delta\right]},$$

where  $\Delta$  and  $\delta$  represent the contributions of uniaxial field and spin-orbit interaction, respectively, to the splittings  $E_{1,2}$  and  $E_{2,3}$ . Having observed the excited-state transitions in emission from the  $A$  and  $B$  bands, one can make a determination of the band-gap energies, the difference of which gives a reliable energy separation of those bands of 0.0095 eV. The difference between the  $B$  and  $C$  exciton transition energies is estimated from the reflection spectra since the  $C$  exciton in emission was not observed. The energies of the reflection minima were taken as the exciton transition energies, realizing that these are not the energy positions of the oscillators. Since we are concerned only with the energy difference, this allows an estimate for the value of  $E_{2,3}$ . Assuming that the binding energies of the  $B$  and  $C$  excitons are reasonably close, this will also be the difference between the  $B$  and  $C$  band gaps. This gives an  $E_{2,3}$  value of 0.0397 eV. Substituting the  $E_{1,2}$  and  $E_{2,3}$  values into the quasicubic model, the spin-orbit and crystal-field parameters can be estimated. Assuming  $\delta < \Delta$ , the spin-orbit parameter is 16 meV, while the crystal-field parameter is 43 meV. One would expect the spin-orbit parameter to be small due to the small atomic number of oxygen. The parameters that have been determined from the exciton spectra of ZnO are compiled in Table II.

### ROTATOR STATES IN ZnO

Defect pair spectra have been observed in the ZnO samples being investigated.<sup>12</sup> This results in a number of PL lines at slightly different energies due to different pair separations. These pairs are not of the usual donor-acceptor nature, but behave simply as neutral-donor complexes; the emission then results from the collapse of excitons bound to the donors. On the high-energy side of the neutral-donor-bound exciton complex lines is a similar set of lines, which are excited states of the lower-energy complex structure. These excited states are analogous to the rotational states of the  $H_2$  molecule. A model for the rotational states was proposed by Rorison *et al.*<sup>13</sup> to explain their high-magnetic-field results in InP. In this model, the donor-bound exciton  $D^\circ, X$  is considered to be a free exciton orbiting a neutral donor; one electron was considered to be strongly correlated with the hole and the other with the donor. Some of the rotator states associated with the defect-donor-bound excitons in ZnO are shown in Fig. 5, along with the free-exciton transitions. These transitions are shown for  $E \perp c$  in zero-magnetic field, and for an applied magnetic field oriented  $H \perp c$  and

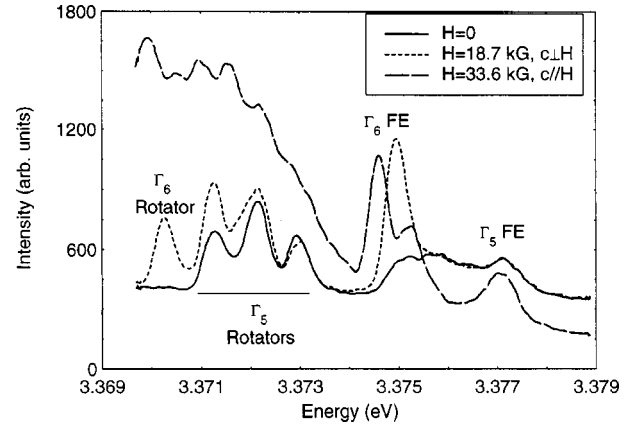


FIG. 5. The  $\Gamma_5$  and  $\Gamma_6$  free exciton transitions along with several donor-bound exciton rotator state transitions. These transitions are shown in zero field and with applied fields in the orientations  $H \perp c$  and  $H \parallel c$ . In zero magnetic field the lowest energy  $\Gamma_5$  rotator state occurs at 3.3714 eV. In an applied magnetic field ( $H \perp c$ ), the lowest energy  $\Gamma_6$  rotator state occurs at 3.3702 eV. In an applied magnet field of 33.6 kG ( $H \parallel c$ ), the split components of the  $\Gamma_6$  free exciton occur at 3.3752 and 3.3746 eV, and the split components of the  $\Gamma_6$  rotator state occur at 3.3704 and 3.3698 eV.

$H \parallel c$ . In zero-magnetic field, the  $\Gamma_5$  free exciton as well as the  $\Gamma_5$  exciton associated with  $D^\circ, X$  rotator states are observed. When  $H \perp c$  is turned on, the  $\Gamma_6$  free exciton as well as the  $\Gamma_6$  exciton associated with the rotator state appear. The 3.3702 eV  $\Gamma_6$  rotator state and the 3.3714 eV  $\Gamma_5$  rotator state are associated with the 3.3594 eV  $D^\circ, X$  transition, not shown here but reported in Ref. 13. When  $H \parallel c$  is turned on, both the  $\Gamma_6$  free exciton and the  $\Gamma_6$  rotator state show a magnetic-field splitting. Assuming the unallowed  $\Gamma_6$  excitons were  $\Gamma_2$  excitons they would not be expected to split in a magnetic field since the  $\Gamma_2$  is a singlet exciton. This is consistent with a  $\Gamma_7 \times \Gamma_9$  transition rather than a  $\Gamma_7 \times \Gamma_7$  transition. It is seen in Fig. 5 that the  $\Gamma_6$  free exciton and the  $\Gamma_6$  rotator exciton show essentially the same magnetic-field splitting. Additional splittings are observed on the high-energy side of the 3.3702 eV  $\Gamma_6$  rotator state. These result from  $\Gamma_6$  excitons associated with other donor-bound excitons, where the  $\Gamma_6$  rotators are masked by  $\Gamma_5$  rotators associated with different  $D^\circ, X$  lines in zero field (Ref. 13).

### CONCLUSIONS

We have observed that the unallowed free-exciton transition, associated with the top valence band in ZnO as well as the same exciton associated with rotator states, splits in an applied magnetic field. The magnitude of the magnetic-field splitting of the unallowed exciton, both as a free exciton and as an exciton in a rotator state associated with a neutral donor, was measured. A  $g$  value of 3.09 was obtained, and this value is the sum of the electron and hole- $g$  values. This is the predicted splitting for the  $\Gamma_6$  exciton from effective mass and group theory.<sup>4</sup> We therefore associate the top valence band with  $\Gamma_9$  symmetry. By superimposing the emission and reflection spectra, we associate the  $A$ -band free exciton with the transition originally reported by Thomas.<sup>2</sup>

We have observed the excitons associated with the  $A$  and  $B$  bands in emission. In the case of the  $A$  band, the  $n = 1, 2,$

and 3 states of the  $\Gamma_5$  and  $\Gamma_6$  excitons were observed, and for the  $B$  band,  $n=1$  and 2 states of the exciton were observed. From these transitions the binding energies of the excitons were determined as well as the band gap energies. From the band-gap energies the energy separation of the  $A$  and  $B$  bands was obtained. The exciton associated with the  $C$  band was not observed in emission, and as a result, the position of the oscillator associated with the  $C$  band was not determined. Based on the energy separation of the reflection minima for the  $B$  and  $C$  bands and assuming the exciton binding energies for the two bands to be similar, the energy separation of the  $B$  and  $C$  bands was estimated. From the band separations an

estimate of the spin-orbit and crystal-field parameters is given in Table II.

#### ACKNOWLEDGMENTS

The authors would like to thank C. Huang for technical support. The work of D.C.R., D.C.L., and B.J. was performed at Wright-Patterson Air Force Base under USAF Contract No. F33615-95-C-1619. This work was partially supported by the Air Force Office of Scientific Research (AFOSR).

---

<sup>1</sup>J. L. Birman, Phys. Rev. Lett. **2**, 157 (1959).

<sup>2</sup>D. G. Thomas, J. Phys. Chem. Solids **15**, 86 (1960).

<sup>3</sup>Y. S. Park, C. W. Litton, T. C. Collins, and D. C. Reynolds, Phys. Rev. **143**, 512 (1966).

<sup>4</sup>J. J. Hopfield, J. Phys. Chem. Solids **15**, 97 (1960).

<sup>5</sup>J. J. Hopfield and D. G. Thomas, Phys. Rev. **122**, 35 (1961).

<sup>6</sup>D. C. Reynolds and T. C. Collins, Phys. Rev. **185**, 1099 (1969).

<sup>7</sup>K. Kawabe, R. H. Tredgold, and Y. Inuishi, Electr. Eng. Jpn. **87**, 62 (1967).

<sup>8</sup>G. A. Slack, J. Phys. Chem. Solids **34**, 321 (1973).

<sup>9</sup>G. A. Slack and T. F. McNelly, J. Cryst. Growth **34**, 263 (1976).

<sup>10</sup>S. Adler and J. Birman, GTE Laboratory report (unpublished).

<sup>11</sup>M. Balkanski and J. Des Cloizeaux, J. Phys. Radium **21**, 825 (1960).

<sup>12</sup>D. C. Reynolds, D. C. Look, B. Jogai, C. W. Litton, T. C. Collins, W. Harsch, and G. Cantwell, Phys. Rev. B **57**, 12 151 (1998).

<sup>13</sup>J. Rorison, D. C. Herbert, P. J. Dean, and M. S. Skolnick, J. Phys. C **17**, 6453 (1984).